Evaluation of Intraaneurysmal Blood Velocity by Time-Density Curve Analysis and Digital Subtraction Angiography

Hiroshi Tenjin, Fumio Asakura, Yoshikazu Nakahara, Keigo Matsumoto, Takamasa Matsuo, Fumihiro Urano, and Satoshi Ueda

PURPOSE: **Our purpose was to evaluate intraaneurysmal blood velocity by using time-density curve analysis and digital subtraction angiography.**

METHODS: **In 31 aneurysms, aneurysmal blood velocity was examined with digital subtraction angiography to determine mean transit time (MTT), peak density time (time to peak opacification) (PDT), and time to half-peak opacification (T½). Thirty frames per second were acquired, and the time-density curve was calculated. Regions of interest were drawn on the proximal parent artery, on the distal parent artery, and on the aneurysm itself.**

RESULTS: **There was no significant difference in MTT of blood velocity in the proximal site on the parent artery, in the distal site on the parent artery, and in the aneurysm. Similarly, there was no significant difference in PDT in the parent artery, in the distal site on the parent artery, and in the aneurysm; nor was there a significant difference in T½ in the parent artery, in the distal site on the parent artery, and in the aneurysm; that is, intraaneurysmal blood velocity was similar to that in the parent artery. PDT and T½ of small aneurysms were faster than that of large aneurysms; that is, blood velocity of small aneurysms was faster than that of large aneurysms.**

CONCLUSION: **Intraaneurysmal blood velocity in small aneurysms is similar to that in the parent artery; consequently, the central stream probably reaches the aneurysmal wall. Intraaneurysmal blood velocity in large aneurysms appears to be somewhat slower than that in small aneurysms.**

A causative relationship between an increase in blood velocity and formation of a cerebral aneurysm has been suggested (1, 2). Furthermore, a cooperative study has shown that peaks of arterial hypertension can precipitate aneurysmal bleeding (3). Hypertension induces high blood velocity, and blood velocity is related to several biological reactions (4, 5); therefore, estimations of blood velocity may be useful for predicting the natural course of an aneurysm. However, there have been few systematic clinical investigations of these hemodynamic factors. The ability to estimate intraaneurysmal blood velocity in situ might have an impact on patient care (6). Current advances in the electronics industry have facilitated the development and application of a new technology known as digital imaging. Digital subtraction angiography allows evaluation of hemodynamics by accessing rapidly acquired quantitative data (7). In the present study, we evaluated intraaneurysmal blood velocity through the application of time-density curves and digital subtraction angiography.

Methods

Between 1994 and 1996, 31 aneurysms in 29 patients were examined with digital subtraction angiography in regard to aneurysmal blood velocity. Subjects consisted of 10 men and 19 women, 44 to 82 years old. Aneurysmal sites included the anterior communicating artery (n = 2), the internal carotid artery (n = 14), the internal carotid artery bifurcation (n = 1), the middle cerebral artery (n = 10), the basilar artery bifurcation (n = 3), and the superior cerebellar artery/basilar artery (n = 1). Eight patients were examined within 48 hours after subarachnoid hemorrhage while in the other 23 patients, aneurysms were examined in the chronic stage or as unruptured sacs. The size of the aneurysm was estimated by its maximal diameter.

Digital angiography was performed on an Angiorex Super Series (Toshiba, Tokyo, Japan) unit with a pixel matrix of 512 × 512. The tip of the catheter was advanced into the

FIG 1. *A*, Digital subtraction angiogram of an aneurysm in the middle cerebral artery. The size was determined by correcting for magnification.

B, Regions of interest were drawn on the proximal parent artery, on the distal parent artery, and on the aneurysm itself.
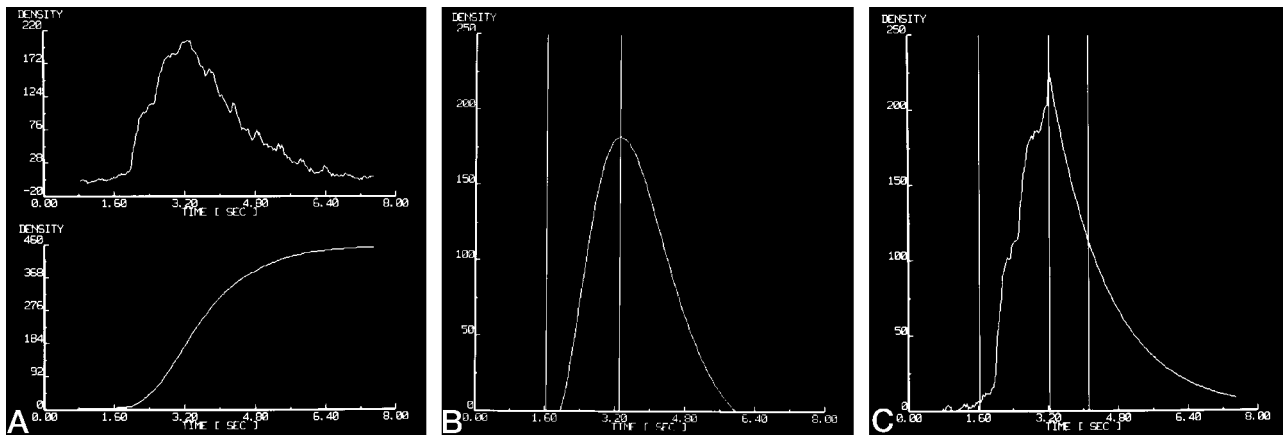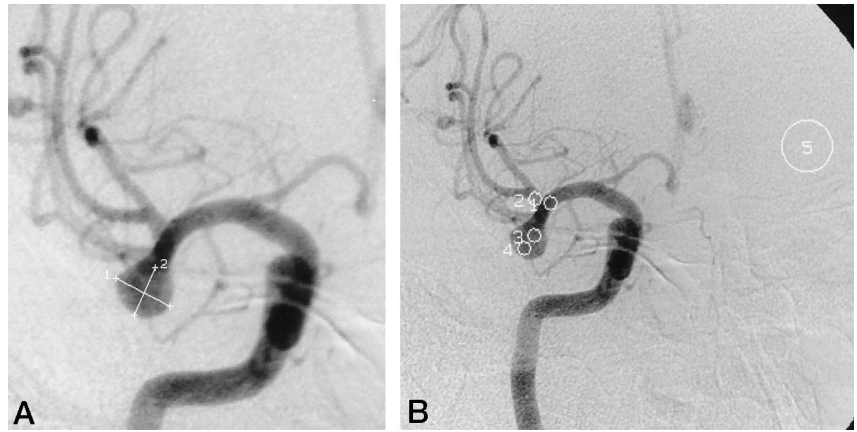

FIG 2.   *A*, Time-density curve (*top*) and integration curve (*bottom*) for contrast medium. The time to half-peak of the integration curve was defined as the mean transit time.

B, The time-density curve was fitted to a γ-variate function, and the peak density time was determined.

C, The time-density curve was fitted to an exponential function, and the time to half-peak was determined.

common carotid artery or vertebral artery, and 4 to 7 mL of contrast medium was delivered at 1.2 to 2.0 mL/s via an automatic pressure injector. Thirty frames per second were acquired for 10 seconds. Projections were chosen that showed the aneurysm in profile and without superimposition of adjacent arteries. Large veins were avoided. Two projections were acquired if possible. Regions of interest (ROIs) were drawn on the proximal parent artery, on the distal parent artery, and on the aneurysm itself. When the aneurysm was large enough to draw several ROIs, they were drawn on the orifice of the aneurysm and on the tip of the aneurysm. The average of the values obtained at the orifice and the tip was used to define the flow of the aneurysm. Each ROI had a diameter of 3 to 5 mm. Because the circle of Willis, where aneurysms are often found, is in the center of the skull, the sella turcica (anteroposterior view) and midline (lateral view) were used as landmarks of the aneurysm. Magnification was determined from the distance between the sella turcica or midline and the image intensifier. The error was less than 0.5 mm (Fig 1).

Blood velocity rates were determined by the time-density curve; that is, by measuring density as contrast medium passed points in the parent artery and aneurysm (7). Time-density curves were obtained in each ROI. To subtract the background density from each frame, we determined the density in the area not perfused by contrast medium. The initial time was defined as the time at which each curve took an upward turn in the ROI of the proximal parent artery, and the entire first-pass curve was established without any recirculation. Mean transit time

(MTT) was determined as $\Sigma(0-\infty)Ct/\Sigma(0-\infty)C$, where C is the quantity of contrast medium remaining at the site (Fig 2A) (8). The time-density curve was fitted by the γ-variate function. The time to peak opacification was defined as peak density time (PDT) (Fig 2B), and the time to half-peak opacification (T½) was defined as the time from peak opacification to half washout of contrast medium (Fig 2C) (9).

Blood velocity studies were evaluated as follows: 1) the difference between ROIs on the proximal site of the parent artery, on the distal site of the parent artery, and on the aneurysm; 2) the difference between ROIs in the aneurysmal orifice and in the tip of the aneurysm; 3) the difference between acute and chronic cases (acute cases were those observed within 48 hours after the onset of subarachnoid hemorrhage, while chronic cases were those examined in the chronic stage or as unruptured aneurysms); 4) the difference between side-wall and bifurcation aneurysms (side-wall aneurysms included those in the internal carotid artery–ophthalmic artery, the internal carotid artery–posterior communicating artery, and the basilar artery–superior cerebellar artery, while bifurcation aneurysms included those in the internal carotid artery bifurcation, middle cerebral artery, anterior communicating artery, and basilar artery bifurcation); and 5) the difference between small and large aneurysms (small aneurysms were defined as those less than 10 mm in diameter, while large aneurysms were greater than 10 mm in diameter) (10). Analysis of variance (ANOVA) was used to assess differences. A *P* value of less than .05 was considered significant.

TABLE 1: Average blood velocity in the proximal site of the parent artery, in the distal site of the parent artery, and in the aneurysm

	Blood Velocity Rates, s		
	Proximal Site of Parent Artery	Distal Site of Parent Artery	Aneurysm
MTT	1.82 ± 0.39	2.09 ± 0.51	1.91 ± 0.44
PDT	1.39 ± 0.31	1.56 ± 0.37	1.53 ± 0.38
T½	0.64 ± 0.26	0.93 ± 0.53	0.83 ± 0.52

Note.—MTT, mean transit time; PDT, time to peak opacification; T½, time to half-peak. Differences were not significant.

TABLE 2: Average blood velocity in two regions of interest in the aneurysm

	Blood Velocity Rates, s	
	Aneurysmal Orifice	Aneurysmal Tip
MTT	1.88 ± 0.45	1.88 ± 0.44
PDT	1.56 ± 0.43	1.55 ± 0.40
T½	0.88 ± 0.45	0.89 ± 0.55

Note.—MTT, mean transit time; PDT, time to peak opacification; T½, time to half-peak. Differences were not significant.

Results

Difference between ROIs on the Proximal Site of the Parent Artery, on the Distal Site of the Parent Artery, and on the Aneurysm (Table 1)

The MTT on the proximal site of the parent artery was 1.82 seconds ± 0.39, on the distal site of the parent artery MTT was 2.09 ± 0.51, and on the aneurysm MTT was 1.91 ± 0.44. The PDT in the parent artery was 1.39 ± 0.31, the PDT in the distal site on the parent artery was 1.56 ± 0.37, and the PDT in the aneurysm was 1.53 ± 0.38. The T½ in the parent artery was 0.64 ± 0.26, the T½ in the distal site on the parent artery was 0.93 ± 0.53, and the T½ in the aneurysm was 0.83 ± 0.52. There were no significant differences.

Difference between ROIs in the Aneurysmal Orifice and in the Tip of the Aneurysm (Table 2)

The MTT in the aneurysmal orifice was 1.88 ± 0.45, and that in the tip of the aneurysm was 1.88 ± 0.44. The PDT in the aneurysmal orifice was 1.56 ± 0.43, and that in the tip of the aneurysm was 1.55 ± 0.40. The T½ in the aneurysmal orifice was 0.88 ± 0.45, and that in the tip of the aneurysm was 0.89 ± 0.55. There were no significant differences.

Difference between Acute and Chronic Cases (Table 3)

The MTT in acute cases was 1.85 ± 0.22, and that in chronic cases was 1.92 ± 0.50. The PDT in acute cases was 1.50 ± 0.10, and that in chronic cases was 1.54 ± 0.45. The T½ in acute cases was 0.90 ± 0.35, and that in chronic cases was 0.83 ± 0.51. There were no significant differences.

TABLE 3: Average blood velocity in acute and chronic cases

	Blood Velocity Rates, s	
	Acute Cases (n = 8)	Chronic Cases (n = 23)
MTT	1.85 ± 0.22	1.92 ± 0.50
PDT	1.50 ± 0.10	1.54 ± 0.45
T½	0.90 ± 0.35	0.83 ± 0.51

Note.—MTT, mean transit time; PDT, time to peak opacification; T½, time to half-peak. Differences were not significant.

TABLE 4: Average blood velocity in side-wall aneurysms and bifurcation aneurysms

	Blood Velocity Rates, s	
	Side-Wall Aneurysms (n = 15)	Bifurcation Aneurysms (n = 16)
MTT	1.86 ± 0.55	1.95 ± 0.32
PDT	1.58 ± 0.51	1.48 ± 0.21
T½	0.83 ± 0.59	0.86 ± 0.35

Note.—MTT, mean transit time; PDT, time to peak opacification; T½, time to half-peak. Differences were not significant.

TABLE 5: Average blood velocity in small aneurysms and large aneurysms

	Blood Velocity Rates, s	
	Small Aneurysms (n = 24)	Large Aneurysms (n = 7)
MTT	1.86 ± 0.42	2.09 ± 0.52
PDT	1.45 ± 0.30	1.81 ± 0.53
T½	0.75 ± 0.31	1.16 ± 0.77

Note.—MTT, mean transit time; PDT, time to peak opacification; T½, time to half-peak. There was a slight but insignificant difference in MTT; there was a significant difference in PDT ($P = .023$) and in T½ ($P = .038$).

Difference between Side-Wall and Bifurcation Aneurysms (Table 4)

The MTT in side-wall aneurysms was 1.86 ± 0.55, and that in bifurcation aneurysms was 1.95 ± 0.32. The PDT in side-wall aneurysms was 1.58 ± 0.51, and that in bifurcation aneurysms was 1.48 ± 0.21. The T½ in side-wall aneurysms was 0.83 ± 0.59, and that in bifurcation aneurysms was 0.86 ± 0.35. There were no significant differences.

Difference between Small and Large Aneurysms (Table 5)

The MTT in small aneurysms was 1.86 ± 0.42, and that in large aneurysms was 2.09 ± 0.52; this was a slight but not significant difference. The PDT in small aneurysms was 1.45 ± 0.30, and that in large aneurysms was 1.81 ± 0.53; this was a significant difference ($P = .023$). The T½ in small aneurysms was 0.75 ± 0.31, and that in large aneurysms was 1.16 ± 0.77; this was also a significant difference ($P = .038$). Blood velocity in large aneurysms was slower than that in small aneurysms.

Discussion

Increased blood flow has been linked to formation of cerebral aneurysms; for example, years after ligation of the cervical carotid artery, aneurysms of the contralateral intracranial carotid artery have been known to develop (1, 2). Moreover, high shear stress may induce intramural aneurysmal hemorrhage (11).

With the use of digital subtraction angiography, blood velocity rates may be determined by calculating time-density curves based on measurements of density obtained as contrast medium passes specific points in the vessel (7). Formulas by which MTT, PDT, and T½ are determined are commonly used to measure tissue blood flow (9). Because contrast medium (iopamidol) is effectively dispersed instantaneously, the same formula is applicable. Errors in measuring flow in a phantom tube and in experimental animals with this technique are approximately 10% (12–15). Flow measurements obtained with an electromagnetic flow probe correlate with measurements obtained with this method (16, 17); therefore, we think it is reasonable to use this technique for clinical investigation.

In vitro experiments have shown various relationships between hemodynamic forces and cerebral aneurysms. In glass models, a correlation between aneurysmal shape and flow pattern has been reported (5, 18, 19). High-velocity central streams appear to reach the aneurysmal wall (18, 20–22). In the present study, no difference in blood velocity pattern was found between the parent artery and the aneurysm, as demonstrated by the time-density curve on digital subtraction angiograms. This result is compatible with prior experimental findings. Since high-velocity central streams must reach the aneurysm, intraaneurysmal blood velocity is similar to the pattern in the parent artery. However, turbulence in human intracranial saccular aneurysms has been detected by phonocatheter (23), suggesting that some secondary flow is induced in the aneurysm even if a central stream reaches the aneurysmal wall.

Our study also revealed no difference in flow velocity between side-wall aneurysms and bifurcation aneurysms. Niimi et al (18) suggested that sheer stress was greater at the outer side wall along the curvature of vessels. Usually, side-wall aneurysms exist on the outer side wall along the curvature of vessels; thus, the central stream probably reaches the aneurysm not only in bifurcation aneurysms but also in side-wall aneurysms.

In large aneurysms, factors related to the time-density curve show prolongation, suggesting that vortex flow is induced in the aneurysm. Niimi et al (18) showed that secondary flow was promoted between the main stream and the vortex flow in a glass aneurysmal model. Other glass-model studies have also shown that circulation in large lobular aneurysms is not rapid (19). This finding seems paradoxical to findings that large aneurysms rupture more often than small ones (10, 24). However, Ferguson and coworkers (20, 25) demonstrated that increases in size are associated with thinning of the wall, thus increasing stress according to the law of Laplace. Flow in the large aneurysms must maintain a fine balance. Jet flow into a large aneurysm may also be an important factor for rupture, and has been demonstrated in experimental aneurysms; however, the digital subtraction angiographic apparatus at our institute could not detect it (26). Better resolution is required to analyze aneurysmal blood velocity in detail.

Conclusion

Intraaneurysmal blood velocity in small aneurysms is similar to that in the parent artery; consequently, the central stream probably reaches the aneurysmal wall, not only in bifurcation aneurysms but also in side-wall aneurysms. Intraaneurysmal blood velocity in large aneurysms appears to be somewhat slower than that in small aneurysms.

Acknowledgments

References

1. Hashimoto N, Kim C, Kikuchi H, Kojima M, Kang Y, Hazama F. **Experimental induction of cerebral aneurysms in monkeys.** *J Neurosurg* 1987;67:903–905
2. Salar G, Mingrino S. **Development of intracranial saccular aneurysms: report of two cases.** *Neurosurgery* 1981;8:462–465
3. Locksley HB. **Report on the co-operative study of intracranial aneurysms and subarachnoid hemorrhage. Section V, part 1: Natural history of subarachnoid hemorrhage, intracranial aneurysms and arteriovenous malformations.** *J Neurosurg* 1966;25:219–239
4. Franke RP, Grafe M, Schnittler H, Mittermayer C. **Induction of human vascular endothelial stress fibers by fluid shear stress.** *Nature* 1984;307:648–649
5. Nemerson Y, Turitto VT. **The effect of flow on hemostasis and thrombosis.** *Thromb Haemost* 1991;66:272–276
6. Tenjin H, Ueda S, Nakahara Y, Masaki H, Matsuo T. **Estimation of aneurysm blood flow: an aneurysm embolized using detachable coil.** *Neurosurg Lett* 1995;5:119–122
7. Hoffmann KR, Lipton MJ. **Digital imaging of the cardiovascular system.** In: Grainger RG, Allison D, eds. *Grainger & Allison's Diagnostic Radiology.* New York: Churchill Livingstone; 1997:619–629
8. Zierler KL. **Equations for measuring blood flow by external monitoring of radioisotopes.** *Circ Res* 1965;16:309–321
9. Merrick MV. **Xenon, red cell and transit time methods for cerebral blood flow measurement.** In: Murray IPC, Ell PJ, Strauss HW, eds. *Nuclear Medicine in Clinical Diagnosis and Treatment.* New York: Churchill Livingstone; 1994:535–548
10. Wiebers DO, Whisnant JP, Sundt TM Jr. **The significance of unruptured intracranial saccular aneurysms.** *J Neurosurg* 1987;66:23–29
11. Schubiger 0, Valavanis A, Wichmann W. **Growth-mechanism of giant intracranial aneurysms: demonstration by CT and MR imaging.** *Neuroradiology* 1987;29:266–271
12. Bursch JH, Hahne HJ, Brennecke R, Gronemeier D, Heintzen PH. **Assessment of arterial blood flow measurements by digital angiography.** *Radiology* 1981;141:39–47
13. Forbes G, Gray JE, Felmlee JP. **Phantom testing of peripheral artery: absolute blood flow measurement with digital arteriography.** *Invest Radiol* 1985;20:186–192
14. Link DP, Lantz BMT, Foerster JM, Holcroft JW, Reid MH. **New videodensitometric method for measuring renal artery blood flow at routine arteriography: validation in the canine model.** *Invest Radiol* 1979;14:465–470

15. Smith HC, Frye RL, Donald DE, et al. **Roentgen videodensitometric measure of coronary blood flow.** *Mayo Clin Proc* 1971;46:800–806

16. Fencil LE, Doi K, Chua KG, Hoffman KR. **Measurement of absolute flow rate in vessels using a stereoscopic DSA system.** *Phys Med Biol* 1989;34:659–671

17. Lantz BM, Foerster JM, Link DP, Holcroft JW. **Determination of relative blood flow in single arteries: new video dilution technique.** *AJR Am J Roentgenol* 1980;134:1161–1168

18. Niimi H, Kawano Y, Sugiyama I. **Structure of blood flow through a curved vessel with an aneurysm.** *Biorheology* 1984;21:603–615

19. Roach MR, Scott S, Ferguson GG. **The hemodynamic importance of the geometry of bifurcations in the circle of Willis (glass model studies).** *Stroke* 1972;3:255–267

20. Ferguson GG. **Physical factors in the initiation, growth, and rupture of human intracranial saccular aneurysms.** *J Neurosurg* 1972; 37:666–677

21. Karino T, Motomiya M. **Flow visualization in isolated transparent natural blood vessels.** *Biorheology* 1983;20:119–127

22. Karino T, Takeuchi S, Kobayashi N, Motomiya M, Mabuchi S. **Fluid dynamics in cerebrovascular disorders.** *Neurosurgery* 1993; 12:15–24

23. Ferguson GG. **Turbulence in human intracranial saccular aneurysms.** *J Neurosurg* 1970;33:485–497

24. Yamamoto K, Tenjin H, Nakahara Y, et al. **Surgical indication for unruptured aneurysm.** *J Kyoto Pref Univ Med* 1996;105:485–490

25. Canham PB, Ferguson GG. **A mathematical model for the mechanics of saccular aneurysms.** *Neurosurgery* 1985;17:291–295

26. Asakura F, Nakahara Y, Matsumoto K, Tenjin H, Ueda S. **Estimation of aneurysmal blood flow: investigation of the flow in experimental aneurysm.** *J Kyoto Pref Univ Med* 1997:106:1–6